Fusogenic Domains of Golgi Membranes Are Sequestered into Specialized Regions of the Stack that Can Be Released by Mechanical Fragmentation

Michel Dominguez,* Ali Fazel,* Sophie Dahan,* Jacque Lovell,‡ Louis Hermo,* Alejandro Claude,‡ Paul Melançon,‡ and J.J.M. Bergeron*

*Department of Anatomy and Cell Biology, McGill University, Montreal, Quebec, Canada, H3A 2B2; and ‡Department of Cell Biology, University of Alberta, Edmonton, Alberta, Canada T6G 2H7

Abstract. A well-characterized cell-free assay that reconstitutes Golgi transport is shown to require physically fragmented Golgi fractions for maximal activity. A Golgi fraction containing large, highly stacked flattened cisternae associated with coatomer-rich components was inactive in the intra-Golgi transport assay. In contrast, more fragmented hepatic Golgi fractions of lower purity were highly active in this assay. Control experiments ruled out defects in glycosylation, the presence of excess coatomer or inhibitory factors, as well as the lack or consumption of limiting diffusible factors as responsible for the lower activity of intact Golgi fractions. Neither Brefeldin A treatment, preincubation with KCl (that completely removed associated coatomer) or preincubation with imidazole buffers that caused unstacking, activated stacked fractions for transport. Only physical fragmentation promoted recovery of Golgi fractions active for transport in vitro. Rate-zonal centrifugation partially separated smaller transport-active Golgi fragments with a unique v-SNARE pattern, away from the bulk of Golgi-derived elements identified by their morphology and content of Golgi marker enzymes (*N*-acetyl glucosaminyl and galactosyl transferase activities). These fragments released during activation likely represent intra-Golgi continuities involved in maintaining the dynamic redistribution of resident enzymes during rapid anterograde transport of secretory cargo through the Golgi in vivo.

Key words: protein transport • Golgi • vesicular transport • secretion

SEVERAL mechanisms have been proposed to describe transport of protein cargo through the Golgi apparatus, but the apparent complexity of the process has so far prevented a clear resolution (Mellman and Simons, 1992; Griffiths, 1996; Bannykh and Balch, 1997; Schekman and Mellman, 1997; Farquhar and Palade, 1998; Pelham, 1998). The "vesicular" transport model argues that the Golgi apparatus is comprised of several distinct subcompartments and that transfer of cargo through these stable subcompartments involves successive vesicular transport steps (Palade, 1975, 1983; Rothman and Orci, 1992; Rothman, 1996; Rothman and Wieland, 1996; Schekman and Mellman, 1997). Alternatively, it has been proposed that the Golgi stack is a single dynamic organelle made up of subdomains capable of fission and homotypic fusion events (Ho et al., 1990; Mellman and Simons, 1992; Clermont et al., 1994), possibly involving transient tubular connections (Weidman, 1995; Mironov et al., 1997; Lippincott-Schwartz et al., 1998). Revised "cisternal maturation" models in which cisternae are formed de novo and progressively mature by vesicle-mediated selective retrieval of Golgi resident enzymes have also been put forward (Schnepf, 1993; Bannykh and Balch, 1997; Gaynor and Emr, 1997; Glick et al., 1997; Bonfanti et al., 1998; Love et al., 1998; Pelham, 1998).

The biochemical machinery for transport through the Golgi complex has been elucidated in part from cell-free studies based on an assay that has been proposed to reconstitute transport of cargo between cis and medial Golgi compartments (Rothman and Orci, 1992; Rothman, 1996; Rothman and Wieland, 1996; Happe and Weidman, 1998). Transport is measured between two distinct Golgi fractions, one isolated from mutant CHO cells lacking the

Drs. Dominguez and Fazel contributed equally to this work and should be considered co-first authors.

Dr. Dahan's present address is Dept. of Biochemistry & Molecular Biology, Center for Basic Research in Digestive Diseases, Mayo Clinic & Foundation (Gugg. 1701), 200 First St., SW, Rochester, MN 55905. Tel.: (507) 284-0580. Fax: (507) 284-0762. E-mail: dahan.sophie@mayo.edu

Dr. Dominguez's present address is Dept. of Biochemistry & Molecular Biology, Thoracic Diseases Research Unit, Mayo Clinic & Foundation (Gugg. 663), 200 First St., SW, Rochester, MN 55905. Tel.: (507) 266-4455. Fax: (507) 284-4452. E-mail: dominguez.michel@mayo.edu

Address correspondence to Paul Melançon, Dept. of Cell Biology, University of Alberta, Edmonton, Alberta, Canada T6G 2H7. Tel.: (780) 492-6183. Fax: (780) 492-0450. E-mail: paul.melancon@ualberta.ca

Golgi enzyme *N*-acetylglucosamine transferase I (NAGT I),[1] but enriched in a specific membrane protein, the envelope glycoprotein of vesicular stomatitis virus (VSV-G), the other obtained from wild-type cells to provide the missing NAGT I activity (Fries and Rothman, 1980; Balch et al., 1984). It has been proposed that in this assay coatomer protein (COP I) vesicles mediate transfer of cargo (VSV-G) from the mutant membranes, hence termed "donor" fraction, to the NAGT I–containing wild-type (WT) membranes, termed "acceptor," and that this reaction reconstitutes a vesicular mechanism responsible for transport of newly synthesized cargo proteins through the Golgi stack in vivo (Rothman and Orci, 1992; Rothman, 1996). This interpretation is supported by experiments on protein transfer between Golgi stacks both in fused cells (Rothman et al., 1984) and in vitro (Ostermann et al., 1993; Elazar et al., 1994), and is consistent with the observation of numerous vesicles in the vicinity of Golgi apparatus by electron microscopy in situ (Farquhar and Palade, 1981). The recent identification of two different classes of Golgi-associated COP I–coated vesicular structures containing either retrograde cargo (KDEL receptor) or anterograde cargo (proinsulin) in pancreatic endocrine cells further supports the vesicular transport model (Orci et al., 1997).

Several recent observations challenge this view. Reexamination of the mutant and WT membrane fractions by sedimentation velocity has led to the conclusion that the intra-Golgi transport measures primarily the retrograde vesicular transfer of NAGT I into much larger VSV-G–containing cisternae (Love et al., 1998). In brief, these authors established that a small but significant fraction of NAGT I in cell homogenates resided in small structures with sedimentation properties similar to vesicles that appeared responsible for almost all of WT Golgi activity in the assay. In contrast, the bulk of VSV-G modified in the transport assay did not appear in such small structures (vesicles), but rather resided in much larger and easily separated components (Love et al., 1998). Furthermore, NAGT I could be mobilized from large structures into a smaller vesicular fraction in an ADP-ribosylation factor (ARF)– and coatomer-dependent manner. Therefore, rather than mediate transfer of VSV-G to WT Golgi, COP I vesicles were concluded to transfer NAGT I from WT Golgi membranes to the VSV-G–containing cisternae of the mutant Golgi fraction.

Even though discovered largely through the Golgi cell-free transport assay (Melançon et al. 1987; Malhotra et al., 1989; Serafini et al., 1991; Waters et al., 1991), the COP I coat is not required to obtain an assay signal in the in vitro complementation assay: ARF depletion from cytosol is without effect on the cell-free transport assay although the formation of COP I vesicles shows an obligate requirement for ARFs (Taylor et al., 1994; Happe and Weidman, 1998). These latter observations demonstrated that efficient complementation of the glycosylation defect can occur with equal yield and kinetics by a vesicle-independent mechanism. Such mechanisms could include consumption of previously formed transport intermediates present in the Golgi membrane fractions or, alternatively, fusion with a subcompartment originally continuous with Golgi cisternae but liberated during organelle isolation.

Methods were recently developed in our laboratory for the preparation of several hepatic Golgi fractions with different extents of structural integrity that can be used to investigate the mechanism of protein traffic through the Golgi. Here, we report that the most structurally intact Golgi fraction shows significant enrichment in β-COP and ARFs, but is largely inactive in the Golgi cell-free transport assay. We find that fragmentation but not removal of β-COP by high salt washing effectively restores activity and that activity correlates inversely with average cisternal length. Rate zonal centrifugation yields partial separation of fusogenically active Golgi components with a defined content of v-SNARES from the more rapidly sedimenting bulk of glycosyl transferases containing Golgi components. These studies have revealed a Golgi subcompartment that is not normally a free standing separate entity that is required for transport through the Golgi apparatus. This domain may also play a role in the dynamic remodeling of the Golgi apparatus recently visualized by time lapse recording of HeLa cells expressing green fluorescent protein–galactosyl transferase chimeras (Sciaky et al., 1997).

Materials and Methods

Subcellular Fractionation

The Gi fraction was prepared from rat liver homogenates using a motorized Potter-Elvehjem homogenizer (rotating Teflon® pestle at 2,300 rpm) in ice cold 0.25 M sucrose, 4 mM imidazole, pH 7.4, following protocols described previously (Bergeron, 1979; Bergeron et al., 1982).

The GE fraction was isolated from liver homogenates in ice cold 0.25 M sucrose, 5 mM Tris-HCl, pH 7.4, 25 mM KCl, 5 mM $MgCl_2$, 4.5 mM $CaCl_2$ (STKCM) by a variation of the method of Bergeron et al. (1982) and Smith et al. (1986) in which discontinuous, rather than continuous, sucrose gradients were used to obtain Golgi fractions of high protein concentrations without having to resort to pelleting. After filtration through two layers of cheese cloth and centrifugation at 400 g_{max} for 10 min, supernatants were adjusted to 1.15 M sucrose in STKCM and underlaid beneath a discontinuous gradient of 0.95 and 0.4 M sucrose in STKCM. After centrifugation at 200,000 g_{av} for 90 min, Golgi fractions were collected at the 0.4/0.95 M sucrose interface.

The WNG fraction[2] was isolated from 20% liver homogenates in 0.25 M sucrose containing 5 mM Tris-HCl, pH 7.4, and 5 mM $MgCl_2$ (STM). Unless otherwise indicated, all buffers also contained the proteinase inhibitors PMSF (1 mM) and aprotinin (200 U/ml). Instead of the motor driven Teflon® pestle Potter-Elvehjem homogenizer (Thomas Scientific) used to prepare Gi and GE liver homogenates, the homogenates used for isolation of the WNG fraction were prepared after gentle homogenization of finely minced liver with the type B loose pestle of a Dounce homogenizer (12 strokes; Thomas Scientific). After filtration through two layers of cheese cloth, homogenates were routinely incubated at 4°C for 2 h to ensure that microtubules were depolymerized (Borisy et al., 1975). After low-speed centrifugation at 400 g_{max} for 5 min, the supernatant (S1) was saved and the pellet (P1) rehomogenized in half the original volume with five strokes of the type B pestle. After centrifugation at 400 g_{max} for 5 min, the supernatant (S2) was combined with S1 and centrifuged at 1,475 g_{max} for 10 min. The resulting pellet (P2) was combined with P1 and resuspended in 1.22 M sucrose in the above buffer (20% wt/vol original liver wet weight). A continuous gradient in STM of 0.25–1.10 M sucrose was generated above the load zone and centrifuged at 1,200 g_{av} for 30 min, followed by 83,000 g_{av} in the rotor (SW27; Beckman Instruments, Inc.) for 1 h. The band at ~1 cm above the load zone was collected, adjusted to 0.4 M sucrose in STM without proteinase inhibitors, and centrifuged at 1,475

1. *Abbreviations used in this paper:* ARF, ADP-ribosylation factor; BFA, Brefeldin A; COP I, coatomer protein; GalT sp. act., galactosyl transferase–specific activity; NAGT, *N*-acetylglucosamine transferase; VSV-G, envelope glycoprotein of vesicular stomatitis virus; WT, wild-type.

2. Dr. Wei Lai (W) first uncovered that Golgi fractions (G) could be isolated from low-speed pellets traditionally referred to as the nuclear (N) pellet; hence the designation WNG fraction.

g_{max} for 10 min (P3). Final enrichment in large membranes was achieved by two successive rounds of resuspension in 0.25 M sucrose in STM followed by pelleting at 1,475 g_{max} for 10 min. The final pellet was recovered in 0.25 M STM and represented 0.085 ± 0.02% (n = 7) of the homogenate protein.

Cisternal Disruption

The disrupted WNGdis fraction was prepared using methods identical to those used to obtain WNG fractions with the following modifications. After collection of the initial low-speed pellets at 1,475 g_{max} for 10 min (P3, above), these pellets were rehomogenized in 0.25 M sucrose in 4 mM imidazole, pH 7.4, with proteinase inhibitors, and homogenized with 10 strokes of the motor driven Teflon® pestle (2,300 rpm) of a Potter-Elvehjem homogenizer. After pelleting at 1,475 g_{max} for 10 min and the supernatant saved, the pellet was resuspended, rehomogenized, and repelleted once more using the same protocol. The three resulting supernatants were combined and gently pelleted onto a 2 M sucrose cushion by centrifugation at 144,000 g_{av} for 40 min. The pellicle was resuspended in 1.15 M sucrose in 4 mM imidazole buffer, pH 7.4, and underlaid in a sucrose step gradient of 0.95 and 0.4 M buffered sucrose. After centrifugation for 90 min at 200,000 g_{av}, the interface at 0.4/0.95 M sucrose was collected as the WNGdis fraction.

KCl and Imidazole Treatment

The isolated WNG fraction in 0.25 M STM was adjusted to 300 mM KCl and incubated at 150 μg/ml cell fraction protein for 1 h at 4°C. Membranes were recovered by centrifugation through 0.4 M buffered sucrose layered onto a 2-M buffered sucrose cushion at 201,000 g_{av} for 1 h in an SW40 rotor (Beckman Instruments, Inc.). The band at the 0.4/2 M interface was then collected and mixed by gentle resuspension.

For cisternal dissociation of WNG fraction (WNGI), the isolated WNG fraction was incubated at 150 μg cell fraction protein/ml in 4 mM imidazole, pH 7.4, 0.25 sucrose for 1 h at 4°C, and then collected as described above for KCl-treated WNG membranes.

Differential and Rate-zonal Centrifugation of Golgi Fractions

To determine the sedimentation characteristics of Golgi fractions, the different Golgi fractions (Gi, GE, WNG) were adjusted to 0.25 M sucrose in the respective buffers used to isolate each fraction, with 0.5 ml loaded onto a 0.4 M sucrose cushion (buffered as above) (2.0 ml in the SW60 rotor and centrifuged at the indicated $g \cdot$ min). The pelleted fractions were evaluated for their GalT content.

For identification of the fusogenic component of the WNGdis fraction, the fraction was centrifuged at 200,000 g_{max} for 40 min (Ti60 angle rotor; Beckman Instruments, Inc.). The resultant pellet was resuspended in 0.25 M sucrose (4 mM) imidazole buffer, pH 7.4, and 0.6 ml of fraction (1.2–2.3 mg protein/ml) loaded onto a step sucrose gradient (10 [0.5 ml], 15 [0.5 ml], 20 [0.5 ml], 25 [0.5 ml], 30 [0.5 ml], 35 [0.5 ml], and 40% [0.4 ml] [wt:wt] preincubated 2 h at room temperature and 1 h at 4°C) and centrifuged 10 min at 20,000 rpm using the SW60 rotor. Fractions were collected (0.5 ml) and evaluated for their content of total protein, GalT, NAGT, and transport activities.

Exogenous and Endogenous (Freeze-Frame) Glycosylation Assays

The incorporation of UDP-[^{3}H]-GlcNAc into endogenous acceptors was measured as described (Bergeron et al., 1982, 1985). GalT assays were performed as described previously (Bergeron et al., 1982) and, where applicable, the GalT-specific activity expressed in milliunits (nmol gal transferred/min · mg cell fraction protein). NAGT assays were performed as described by Vischer and Hughes (1981) using ovalbumin as acceptor and UDP-^{3}H GlcNAc as sugar donor.

Iodination of ^{125}I-Insulin and Evaluation of Endosomal Contamination

^{125}I-insulin was prepared as described by Frank et al. (1983). To evaluate endosomal contamination, rats were anesthetized with sodium pentobarbital and injected with 5 μCi of [^{125}I]-insulin into the portal vein. 5 min after injection, the animals were killed and the livers were processed for homogenization and subcellular fractionation as described above.

Cell-free Intra-Golgi Transport Assay

CHO Golgi-enriched membrane fractions were isolated from cells grown in suspension and homogenized in 0.25 M sucrose containing 10 mM Tris-HCl, pH 7.4, and proteinase inhibitors, by 12 passages through a steel ball homogenizer (Balch et al., 1984; Balch and Rothman, 1985). CHO acceptor membranes were obtained from wild-type CHO cells (pro-5, American Type Culture Collection [ATCC]), while donor membranes were obtained from lec1 CHO cells (ATCC) 3.5 h after infection with vesicular stomatitis virus, as described by Weidman et al. (1989). CHO cytosol was prepared as described (Balch et al., 1984; Taylor et al., 1992). Protein concentrations were determined by the BCA method (Pierce Chemical Co.) using immunoglobulins as standard or by the Bradford method (Bio-Rad Laboratories) using bovine serum albumin as standard (Bradford, 1976).

Intra-Golgi transport between VSV-G–containing donor and the various NAGT I–containing acceptor membrane fractions was measured as incorporation of UDP-[^{3}H]-GlcNAc into immunoprecipitated VSV-G essentially as described in Taylor et al. (1992), with the exception that all 25-μl assays contained 2 μl donor membranes (0.07–0.1 μg protein) and 2 μl CHO cytosol (1.4 μg protein), and were performed for 60 min at 37°C. For analysis of transport activity in fractions observed after rate-zonal centrifugation, the assay volume was increased to 50 μl while keeping buffer, sucrose, cytosol, and UDP-[^{3}H]-GlcNAc concentration constant; this change accommodated the larger volumes (10 μl) of liver Golgi fraction to be tested. The amount of acceptor membrane present in a given assay varied between experiments and is stated in the figure legends. Control experiments confirmed that all such assays were performed under linear conditions of either substrate addition by donor Golgi fractions and enzyme addition by acceptor Golgi fractions.

Immunoblotting

Protein samples were first separated by SDS-PAGE, and then transferred onto nitrocellulose membranes (Xymotech). The blots were incubated in 5% skim milk in TNT buffer (10 mM Tris-HCl, pH 7.5, 150 mM NaCl, 0.05% Tween-20). Antibodies to β-COP (affinity-purified rabbit antipeptide antibody EAGE, supplied by Drs. T.E. Kreis and J. Lippincott-Schwartz or monoclonal antibody M3A5; Sigma Chemical Co.) and ARF (mouse monoclonal antibody ID9, a gift of Drs. P. Randazzo and R.A. Kahn, NIH, Bethesda, MD) were used at dilutions of 1/1,000. Secondary antibodies conjugated to alkaline phosphatase were used to visualize immunoblots as described by Smith and Fisher (1984). Polyclonal antibodies to GS15 were visualized using chemiluminescence according to the manufacturer's instructions (NEN Life Science Products). Antibodies to GS28 (monoclonal) and Vti-rp2 (polyclonal) were visualized by radioautography after incubation with ^{125}I rabbit anti–mouse antibodies and ^{125}I-labeled goat anti–rabbit, respectively. Quantitation of ^{125}I signals were by Phosphorimager analysis (Fuji Bioimaging). All SNARE antibodies were a kind gift from Dr. Wanjin Hong (Institute of Molecular and Cell Biology, University of Singapore).

Electron Microscopy

Membrane samples for electron microscopy were prepared using the random sampling filtration apparatus of Baudhuin et al. (1967) as described previously (Paiement and Bergeron, 1983; Bergeron et al., 1985). Before filtration on HA 0.45-μm filters (Millipore Corp.), membrane fractions were fixed at 4°C overnight with an equal volume of 5% glutaraldehyde in 100 mM sodium cacodylate buffer at pH 7.4. Post-fixation was effected either with reduced OsO_4 (equal volumes of 4% OsO_4, 4% potassium ferrocyanide) or for visualization of coats with tannic acid followed by uranyl acetate staining (Simionescu and Simionescu, 1976).

Stereology was performed as described by Rabouille et al. (1995a) for the estimation of both cisternal stacking, as well as cisternal lengths. For this analysis, a cisterna was defined as flattened if its length was at least twice its width. Furthermore, flattened cisternae were considered as stacked if the intercisternal space was less than the width of the cisternal lumen over at least 50% of the cisternal length. Flattened cisternal lengths were determined by tracing their length along the central axis of the sectioned lumen.

Results

Structural Integrity of Hepatic Golgi Fractions

Several Golgi fractions with varying degrees of structural

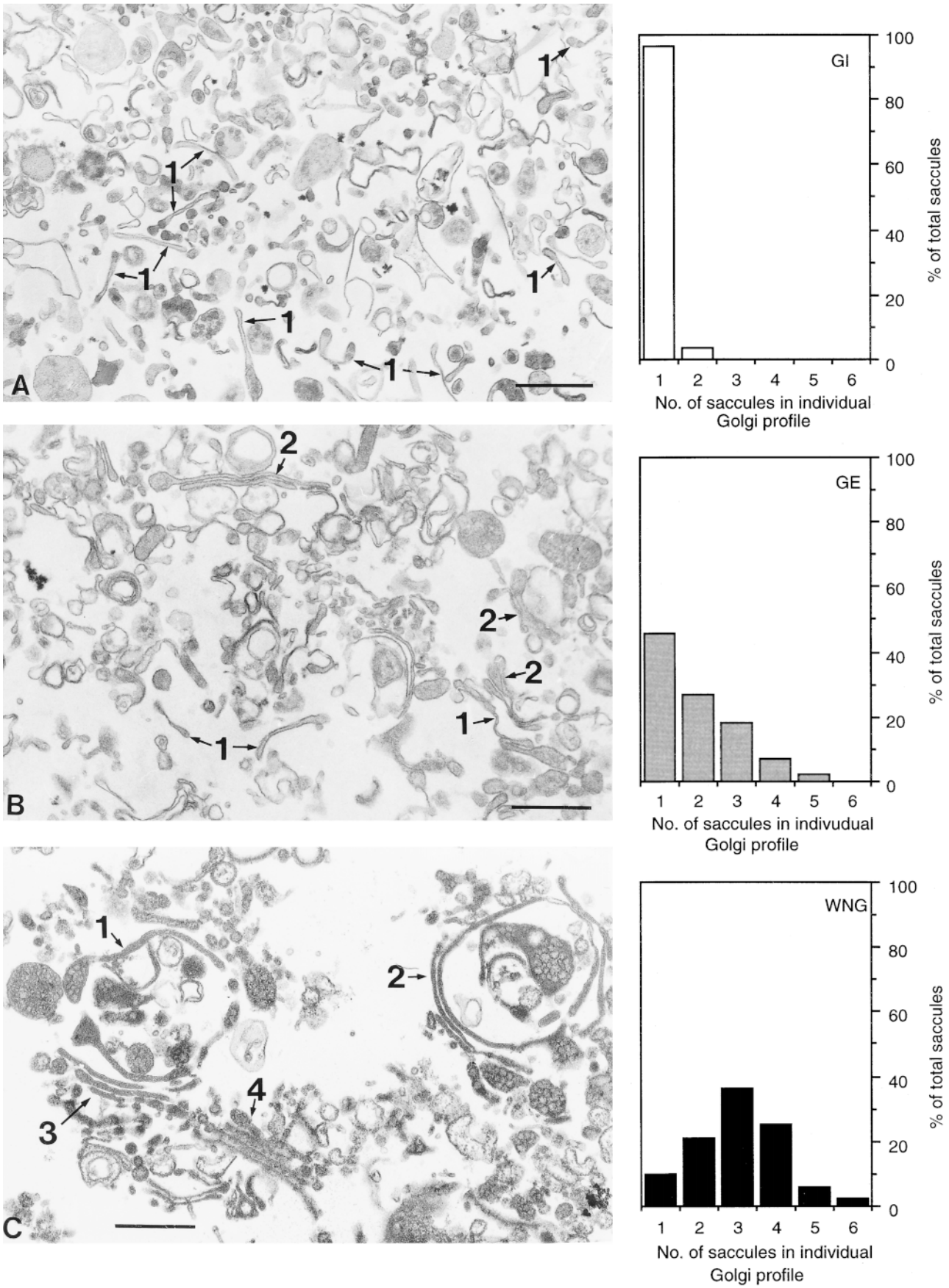

Figure 1. Morphometry reveals Golgi fractions with differing degrees of structural integrity and cisternal stacking. Random sampling of cross sections of the fixed and filtered Golgi fractions; Gi (A), GE (B), and WNG fractions (C). The designation of Golgi apparatus as

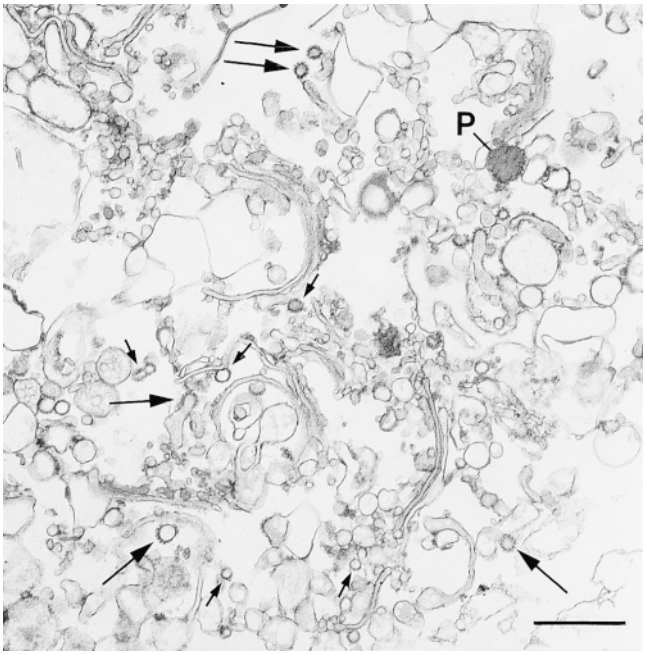

Figure 2. WNG fraction visualized by tannic acid staining. Two types of coats are readily observed: bristle-like (large arrows) and fuzz-coated structures (short arrows) usually of slightly greater diameter than Golgi flattened cisternae. A peroxisomal core contaminant (P) is indicated. Bar, 400 nm.

integrity were prepared using selected buffer conditions, as well as homogenization and centrifugation procedures. The Gi fraction was floated from the high-speed microsomal pellet of hepatic extracts prepared by vigorous homogenization in imidazole buffer (Bergeron, 1979). Electron microscopy of membrane samples recovered by a filtration method that ensures random sampling (Baudhuin et al., 1967) verified that this fraction consisted largely of single Golgi cisternae (Fig. 1 A). Direct floatation from total membrane extracts prepared by vigorous homogenization but in a less disruptive buffer (Tris-HCl containing Mg^{2+}, K^{+}, Ca^{2+}) yielded a fraction (GE fraction; Bergeron et al., 1982) that contained a mixture of stacked and unstacked Golgi cisternae (Fig. 1 B). Finally, a fraction consisting of long Golgi cisternae in a mostly stacked configuration, termed WNG, was isolated after gentler homogenization of liver and floatation from extracts enriched in large structures after their selection by low-speed centrifugation (Fig. 1 C). Tannic acid staining of samples of this WNG fraction further revealed a large number of coated structures (Fig. 2, arrows). Coated structures were not evident in the other fractions (data not shown). The buds in the WNG fraction were generally larger than expected and the intercisternal space considerably narrowed, presumably as a consequence of the staining protocol. Similar results were reported by Orci et al. (1986) in their initial description of COP I–coated vesicles (vesicle diameter/intralumenal space of 3:1).

Table I. Galactosyl Transferase Enrichment and Endosomal Contamination of Hepatic Golgi Fractions

Golgi fraction	GalT (RSA)		NAGT		Endosomal contamination (^{125}I-insulin)	
WNG	160 ± 31	(10)	149 ± 45	(3)	9 ± 6	(3)
GE	74 ± 8	(3)	110 ± 18	(2)	38 ± 11	(3)
Gi	93 ± 31	(3)	120 ± 5	(2)	158 ± 44	(3)

The specific activity of UDP galactose ovomucoid galactosyl transferase (GalT) activity of the WNG fraction was 12.1 ± 0.2 nmols (SD) gal incorporated/min per mg cell fraction protein (n = 10). For UDP *N*-acetyl glucosamine ovalbumin *N*-acetyl glucosaminyl transferase (NAGT), the specific activity of the WNG fraction was 0.64 ± 0.15 nmols (SD) GlcNAc incorporated/min per mg cell fraction protein (n = 3). RSA (relative specific activity) is the enrichment activity of the fraction over the homogenate expressed as the mean ± SD or one-half variation. Endosomal contamination was evaluated by the ^{125}I-insulin content of the Golgi fractions isolated from rats killed at 5 min after the intraportal vein injection of ^{125}I-insulin (80×10^6 cpm, 1 μg) and is expressed as a function of the concentration of ^{125}I-insulin in homogenates as fold enrichment in radioactivity over the concentration of ^{125}I-insulin in the parent homogenates (mean ± SD). The number of separate experiments is indicated in parentheses.

Biochemical characterization of the three preparations established that, despite similar yields, the WNG protocol resulted in significantly greater enrichment of the Golgi markers galactosyl transferase (GalT) and *N*-acetylglucosaminyl transferase (NAGT) (Table I). Furthermore, endosomes, a frequent contaminant of hepatic Golgi fractions, were markedly reduced in the WNG fraction. The highly stacked membranes recovered in the WNG preparation should be representative of the cellular organelle since the yield of the homogenate galactosyl transferase activity (14.5 ± 1.6% (mean ± SD; n = 7)) was similar to that of the Gi and GE fractions (data not shown).

The difference in size of the Golgi components containing the enzyme marker was confirmed by sequential differential centrifugation (Fig. 3). This sedimentation analysis demonstrated that the WNG fraction was the largest with all GalT activity sedimenting completely even under centrifugation conditions as low as 15,700 $g \cdot$ min. By contrast, the GalT marker in the Gi fraction remained completely in the supernatant at 33,680 $g \cdot$ min, and 1.68×10^6 $g \cdot$ min were required to pellet 90% of the GalT activity.

Stacked Hepatic Golgi Fractions Display Low Transport Activity

Previous studies had established that rat liver Golgi preparations can be substituted for the standard Golgi fraction isolated from wild-type CHO cells as a source of NAGT I in the Golgi transport assay (Braell et al., 1984). The three morphologically distinct hepatic Golgi fractions could therefore be compared as a source of NAGT1 for transfer to VSV-G–containing Golgi fractions isolated from a mutant CHO line lacking that activity (Balch et al., 1984). The three hepatic fractions displayed marked differences in the Golgi cell-free transport assay (Fig. 4 A), which appeared inversely related to their size as determined by the

having single cisternae (1), or in stacks of two (2), three (3), or four (4) cisternae is indicated on the micrographs. Bars, 400 nm. Quantitative evaluation (histograms) was based on the analysis of 315 Golgi flattened cisternal profiles of the Gi fraction, 496 profiles of the GE fraction, and 1,617 profiles of the WNG fraction. As seen from the magnification bar, Golgi cisternae are considerably longer in the WNG fraction.

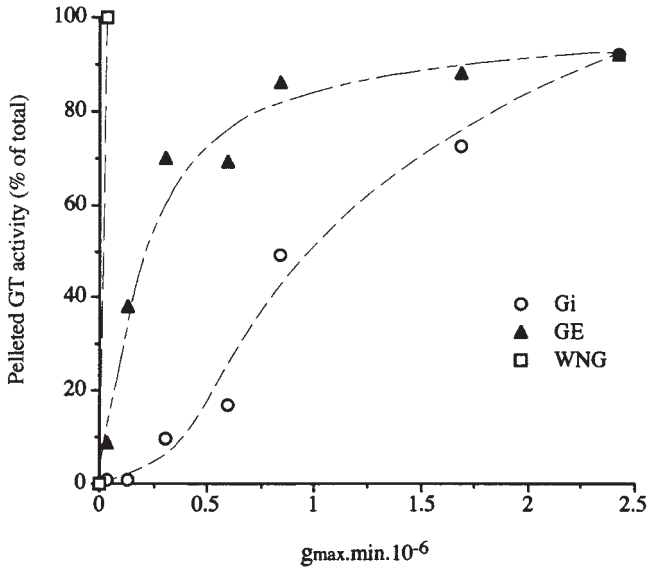

Figure 3. Sedimentation analysis of WNG, GE, and Gi Golgi fractions. The different Golgi fractions (Gi, GE, WNG) were adjusted to 0.25 M sucrose in their respective buffers loaded onto a 2-ml 0.4-M sucrose cushion (buffered) and centrifuged in a SW60 centrifuge rotor under various $g_{max} \cdot$ min conditions by varying time and/or speed. The pelleted fractions were evaluated for their GalT content as described in Materials and Methods.

sedimentation analyses of Fig. 3. The WNG fraction, despite its abundant budding machinery, displayed very low ability to provide NAGT I in the transport-coupled glycosylation assay. In contrast, the unstacked Gi fraction had very high transport activity while the GE fraction displayed an activity similar to the standard acceptor Golgi fraction isolated from wild-type CHO cells (Balch et al., 1984). Note that all assays were performed under linear conditions of transport where neither substrate availability nor enzyme activity were rate limiting.

The differences in transport activity did not result from differential enrichment in Golgi membranes since the inactive WNG fraction showed the highest enrichment in the Golgi marker GalT and NAGT I (Table I). Similarly, the lack of transport activity by the WNG fraction did not result from lack of endogenous substrate accessibility; endogenous glycosylation assays (Bergeron et al., 1985), recently renamed "freeze-frame" glycosylation (Hayes et al., 1993; Hayes and Varki, 1993), established that all three Golgi fractions had a similar ability to transport UDP-[^{3}H]-GlcNAc intraluminally and transfer the sugar to endogenous glycoprotein acceptors using endogenous NAGT I (Fig. 4 B).

The lower activity of the WNG fractions could have been caused by a diffusible inhibitor absent in the other fractions or by the lack and/or consumption of an essential diffusible transport factor. This clearly was not the case, however, since addition of an eight-fold excess of WNG Golgi fraction on a protein basis (or ~15-fold excess by GalT activity) had little effect on the extent of transport, measured with constant amounts (0.25 μg protein) of the most active acceptor Gi fraction (Fig. 4 C). The results of this mixing experiment also eliminated endosomal membranes in the Gi and GE fractions (greatly diminished in the purer WNG fractions, see Table I) as responsible for the higher activity of these preparations since endosomes provided by the Gi fraction did not stimulate the activity of WNG membranes. This was a relevant consideration since COP I coatomer proteins also associate with endosomes (Whitney et al., 1995), thereby potentially complicating in vitro fusion assays.

Finally, if the cis-Golgi network (CGN) contributed to the transport reaction, lower activity could have resulted from selective loss of this compartment during WNG preparation. The Western blot analysis presented in Fig. 4 D demonstrated that this was not the case since p58, a marker of the CGN and the intermediate compartment (Lahtinen et al., 1996), was observed in both Gi and WNG fractions. Furthermore, the cis-Golgi network integral membrane proteins of the p24 family are highly abundant in the WNG fraction (Dominguez et al., 1998). We concluded from these experiments that the explanation for lower activity of the WNG membranes lay elsewhere, possibly in its structural integrity and/or associated proteins.

The Lower Activity of WNG Membranes Does Not Result from the Presence of Excess Coatomer

Previous work has established that addition of GTPγS causes acceptor inactivation, possibly as a consequence of the recruitment of excess coatomer (Melançon et al., 1987; Elazar et al., 1994; Taylor et al., 1994). The abundance of coated structures on WNG membranes described above suggested an examination of the relative ARF and coatomer content of our Golgi fractions. Western blot analysis revealed that WNG membranes contained a high amount of associated β-COP and ARF1 relative to the other hepatic Golgi fractions (Fig. 5, A and B) or to Golgi-enriched membranes obtained from CHO cells (Fig. 5 C).

Several experiments were performed to test the relationship, if any, between the high coatomer content of WNG membranes and their low transport activity. Brefeldin A (BFA) is a small fungal metabolite that interferes with recruitment of COP I coatomer on Golgi membranes (Klausner et al., 1992) and can thus be used to assess the putative role of COP I coatomer in the lower activity of WNG fractions. Fig. 5 C shows that incubation of CHO Golgi membranes in cytosol with or without additional GTPγS dramatically increased β-COP association, but that the WNG fraction appeared nearly saturated with β-COP and showed limited increase after incubations with cytosol. Under these conditions, BFA eliminated β-COP binding to the CHO Golgi fractions and reduced β-COP association with the WNG fraction by nearly 60% (Fig. 5 C). Despite these clear effects of BFA on β-COP association, the drug had a negligible impact on transport reactions containing the inactive WNG fraction (Fig. 5 D). Similarly, BFA did not affect the cell-free transport when NAGT I was provided by Gi (Fig. 5 D) or GE fractions (not shown); each Golgi fraction appeared fixed at its relative ability to serve as enzyme source, independently of BFA addition. We conclude that BFA cannot reactivate the inactive WNG fraction.

KCl treatment has also been found to remove quantita-

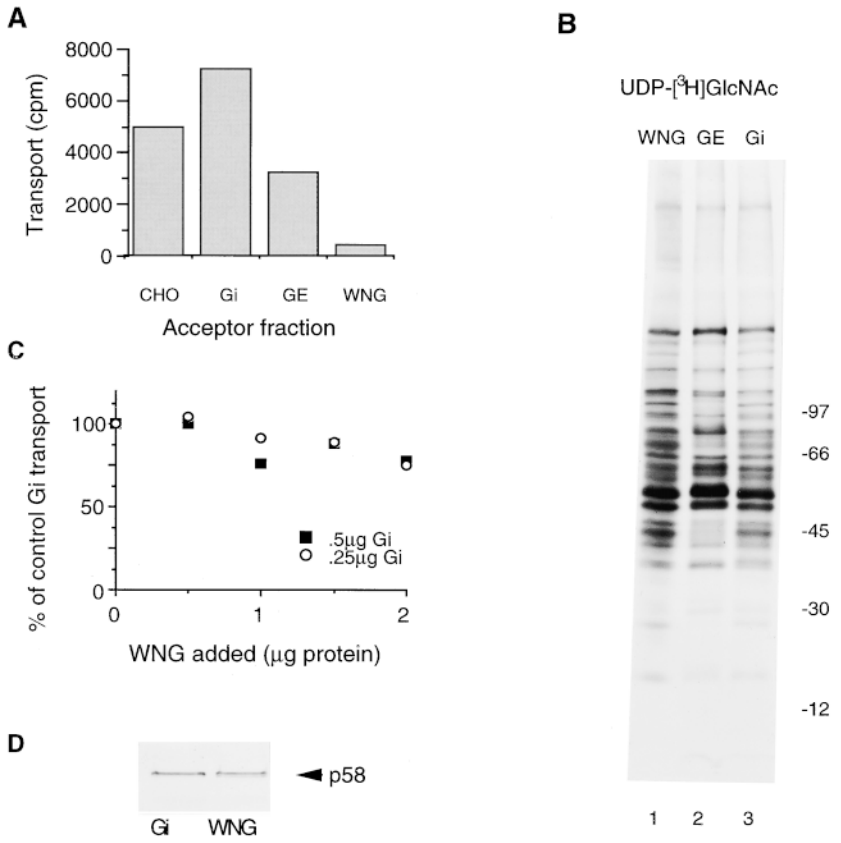

Figure 4. The WNG fraction is a defective acceptor in the Golgi cell-free transport assay. (A) CHO, Gi, GE, and WNG fractions have different acceptor activities. Each 25-μl Golgi cell-free transport assay received identical amounts of Golgi fraction (0.8 μg protein) and the extent of [^{3}H]-GlcNAc incorporated into a specific membrane protein (the VSV-G protein) was determined. Near identical transport activities of the same Golgi fractions were found when BFA was included at 20 μg/ml (not shown). The galactosyl transferase–specific activity (GalT sp. act.) of the Gi, GE, and WNG fractions was 7.6, 10.1, and 24.3 mU, respectively. (B) Glycosylation of endogenous glycopeptide acceptors of Golgi fractions was assessed with UDP-[^{3}H]-GlcNAc as sugar donor and Golgi fractions as endogenous acceptors. Approximately 4 μg cell fraction protein corresponding to ~55,000 dpm of trichloroacetic acid–precipitable radioactivity was applied to each lane and separated on a 5–15% gel by SDS-PAGE. Fluorographic exposure was for 2 mo. Molecular mass markers in kilodaltons are indicated on the right. (C) Mixing experiments reveal that the acceptor WNG fraction neither generates a diffusible inhibitory factor nor consumes a diffusible limiting factor in the Golgi cell-free transport assays. Transport was determined as for A. The indicated amounts of WNG fraction (GalT sp. act., 13.8 mU) were added to transport assays containing either 0.25 (○) or 0.5 (■) μg of the Gi fraction (GalT sp. act., 7.6 mU). (D) An identical amount of Gi and WNG fraction (45 μg protein) was applied to each lane, and p58 content in each fraction was evaluated by immunoblot analysis.

tively β-COP from membrane fractions (Lowe and Kreis, 1995) and was therefore chosen as an alternative to BFA to pursue this question. Incubation with KCl led to the complete removal of β-COP from the WNG fraction (Fig. 5 E). However, complete removal of coatomer did not rescue transport activity since KCl-treated membranes (WNGKCl) displayed no enhanced acceptor activity (Fig. 5 F). Experiments carried out in parallel established that KCl treatment of Gi membranes had no effect on their transport activity (data not shown). These experiments clearly established that the lower activity of the WNG fraction did not result from its elevated COP I coatomer content.

Disruption of Golgi Stacks Rescues Activity in Cell-free Golgi Transport Assays

To test whether simply increasing the amount of accessible membrane by Golgi cisternal unstacking or fragmentation would influence the cell-free transport assay, we developed methods to unstack and disrupt the WNG Golgi membrane fraction. The extent of disruption achieved after various treatments was assessed by differential centrifugation (1,570 g_{max}) under conditions where intact stacks sedimented, and disrupted ones did not (Fig. 3). The distribution of Golgi membranes between pellets and supernatants was measured using GalT as a marker.

Harsh homogenization of the parent low-speed pellet of the WNG fraction revealed a buffer-dependent effect on the release of membrane-bound GalT activity to the supernatant. When the buffer used for rehomogenization was the same sucrose–Tris-$MgCl_2$ buffer used in the initial liver homogenization protocol to prepare the WNG fraction, GalT activity sedimented at low speed (Fig. 6 A). However, changing the homogenization buffer to sucrose-imidazole, the buffer used to isolate the Gi fraction, led to liberation of most of the GalT activity in the low-speed supernatant (Fig. 6 A). Homogenization was only effective when the crude low-speed pellet was used (data not shown). However, organelle fragmentation within the low speed pellet was likely selective for Golgi components since the marked differences in distribution of GalT activity under these conditions were not reflected in the proportion of total protein sedimenting at low speed (Fig. 6 A).

Comparison of Golgi fractions isolated by floatation from parent low-speed pellets rehomogenized in the two different buffers revealed marked differences in their activity as Golgi acceptors. The WNGdis fraction obtained after disruption in imidazole displayed a 3.2-fold higher transport activity than measured with the control WNG fraction (Fig. 6 B). Quantitative evaluation of cisternal unstacking by electron microscopy now revealed a majority of single short cisternae in the WNGdis fraction (50% of all Golgi profiles were single cisternae compared with

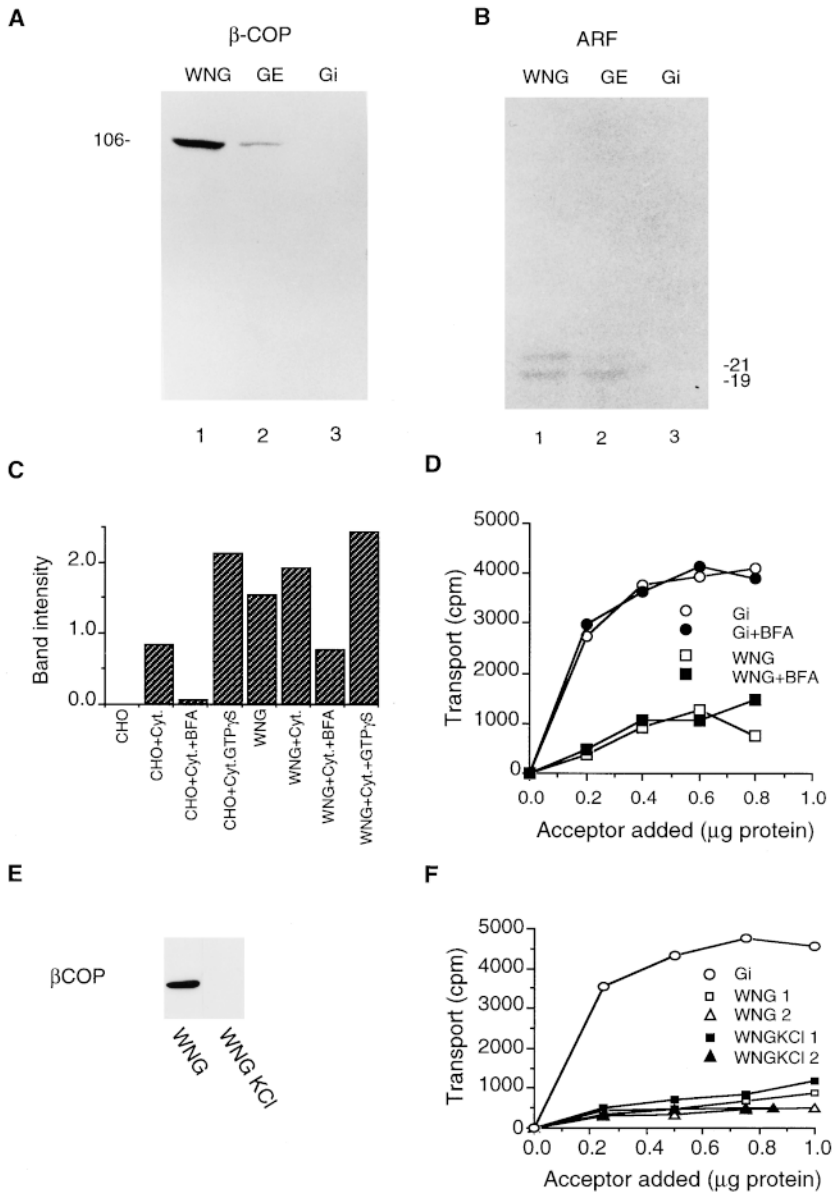

Figure 5. Coatomer is not responsible for the lower activity of WNG membranes. Identical amounts of each Golgi fraction (30 μg) were analyzed for β-COP (A) and ARF (B) content by immunoblot with the polypeptides indicated in kilodaltons. GalT sp. act. of the WNG, GE, and Gi fractions was 11.5, 7.7, and 7.6 mU, respectively. (C) Modulation of β-COP content of Golgi fractions by addition of cytosol, Brefeldin A, and/or GTPγS for 1 h at 37°C, and then pelleted through a sucrose cushion. The extent of membrane-associated β-COP was evaluated by Western blotting, followed by densitometry. The higher level of coatomer in reactions containing WNG membranes likely reflects in part the higher content of Golgi enzymes in those fractions. (D) Brefeldin A does not activate WNG. Transport assays containing the indicated amounts of Gi and WNG fractions were carried out in the presence or absence of 20 μg/ml BFA for 2 h at 30°C. (E) Removal of β-COP by 0.3 M KCl. The β-COP content of the WNG and WNGKCl fractions were evaluated by immunoblotting. Equal amounts of protein (12.5 μg) were applied to each lane. (F) Both WNG and WNGKCl fractions are inactive acceptors. The indicated amounts of Gi, WNG, and WNGKCl were added to assays and the extent of transport in 1 h was determined as described for A. The GalT sp. act. of the WNG fractions was 14.4 and 13.3 mU and for the WNGKCl fractions was 16.3 and 13.3 mU for experiments 1 and 2, respectively.

~10% in the untreated WNG fraction [Fig. 6, C and D]). These experiments demonstrated that disruption of stacked Golgi membranes leads to their activation for transport.

Fragmentation but Not Unstacking Enhances Transport Activity

Further experiments aimed at separating the effects of cisternal unstacking and fragmentation revealed that unstacking was not sufficient for enhanced transport. As shown in Fig. 7, treatment of a WNG fraction in sucrose-imidazole without rehomogenization led to partial cisternal unstacking (Fig. 7, B and C). This did not result in enhanced transport (Fig. 7 A). We therefore concluded that the buffer, but not homogenization, was responsible for cisternal partial unstacking, and that increasing the surface area of cisternal membrane by partial unstacking was not sufficient to enhance transport activity. This result is noteworthy since it suggests an additional approach to characterize some of the molecular interactions leading to the characteristic stacking of Golgi membranes.

To estimate the extent of Golgi fragmentation, we determined the average cisternal lengths in our various Golgi fractions using methods developed by Rabouille et al. (1995a). This analysis confirmed that Golgi fractions obtained after more disruptive homogenization protocols resulted in shorter cisternae (Fig. 8 A). Using the fraction of cisternae with lengths <0.5 μm as a comparative measure, we found a statistically significant correlation ($r = 0.91$) with acceptor activity (Fig. 8 B). This suggests that activation may have resulted from either the release of tethered transport intermediates and/or the fragmentation of cisternae and anastomosing fenestrated elements on the rims of Golgi stacks or intercisternal continuities. Electron microscopy of filtered VSV-G containing CHO Golgi fractions revealed short cisternae (Fig. 8, A and C) that were also unstacked (Fig. 8 D). As shown in Fig. 8 A, these

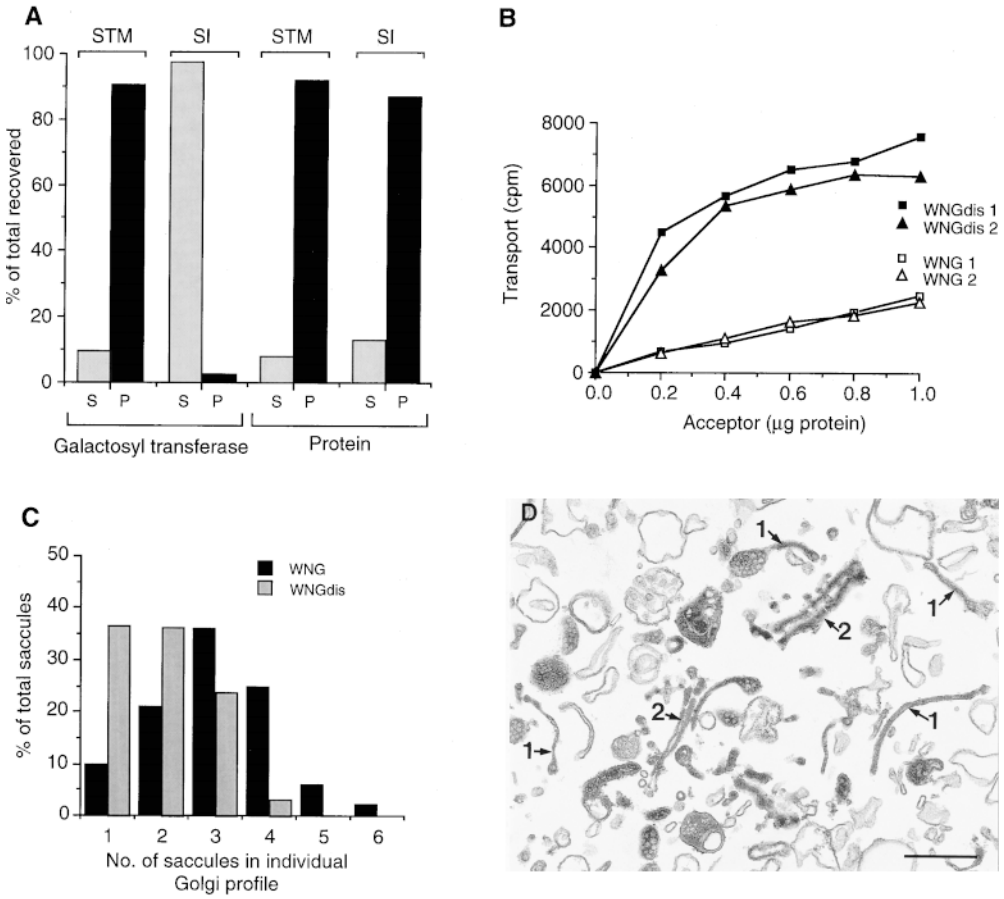

Figure 6. Harsh homogenization in sucrose-imidazole buffer leads to disruption of Golgi structural integrity. (A) The parent low speed pellet (1,570 g_{max} × 10 min) from a WNG preparation was treated with a rotating Teflon® pestle of the Potter-Elvehjem homogenizer in STM or SI buffer. Pellet (P) and supernatant (S) fractions (1,570 g_{max} for 10 min) were analyzed for GalT-specific activity and total protein content. (B) Activation by disruption. Standard WNG fractions and WNG fractions disrupted by harsh homogenization in sucrose-imidazole (WNGdis) were prepared in parallel as described in Materials and Methods. The indicated amounts of the each Golgi fraction were tested for acceptor activity as described for Fig. 4 A. The GalT sp. act. of the WNG fractions were 11.7 and 11.9 mU, while those of the WNGdis fractions were 6.7 and 7.7 mU. The different GalT specific activity of the WNGdis and WNG fractions is likely a consequence of the enhanced protein content liberated as a consequence of the sucrose imidazole treatment (A, right). (C) Electron microscopy reveals that the WNGdis fraction is partially unstacked. Three separate pairs of WNG and WNGdis fractions were fixed and embedded, and the number of cisternae in individual Golgi profiles was assessed. The results shown correspond to the analysis of 122 and 376 profiles for the WNG and WNGdis preparations, respectively. (D) Random view of a filtered WNGdis fraction with single (1) and double (2) saccular profiles indicated. Bar, 400 nm.

CHO Golgi fractions had cisternal lengths comparable in size to those of the rat liver GE fraction, but shorter than the most intact WNG fraction. This observation is in general agreement with the relatively high activity of the CHO membrane preparation when used as source of NAGT I in the Golgi transport assay (Figs. 4 A and 8 B).

Identification of the Fusogenic Compartment by Rate-zonal Centrifugation

The previous analysis established a correlation between appearance of cisternal fragments after harsh homogenization and transport activity, but did not identify the active membranes. To characterize the fusogenically active component in disrupted Golgi fractions and gain insight into the mechanism of activation, we designed sucrose gradients and centrifugation conditions based on data in Fig. 3 that could readily resolve by size small Golgi fragments from partially stacked membranes remaining in the WNGdis fraction (see Materials and Methods for details).

By rate-zonal centrifugation (Fig. 9), the bulk of proteins present in the WNGdis fraction cosedimented with GalT and NAGT I activity as a major peak in fraction 6. In contrast, transport (fusogenic) activity was partially resolved from the peak of GalT and NAGT I activities. Note again that all transport assays were carried out under nonsaturating conditions where signal was proportional to the amount of membrane protein added. Although some transport activity was detected throughout the gradient of Fig. 9, even into fraction 8, the bulk of fusogenic activity was recovered in fractions 1–5. The relatively higher transport activity of structures sedimenting in early fractions is particularly evident when expressed as specific activity relative to protein content (Fig. 10). Electron microscopy of filtered samples from each fraction confirmed the progressive increase in size from fractions 1 to 8 (Fig. 11). Recognizable stacked Golgi cisternae were restricted to fractions 6 and higher, coinciding with the distribution of the bulk of NAGT I and GalT activity (Fig. 9). Vesicular profiles were found throughout the gradient (Fig. 11, arrows), but were only a minority of the pleomorphic structures evident in fractions 1–5 (transport active). Of note were the apparent continuities observed between Golgi cisternae, as well as between cisternal and vacuolar distensions (Fig. 11, panels 6 and 7) in transport-attenuated regions of the gradient.

Since the greater activity of membranes in early frac-

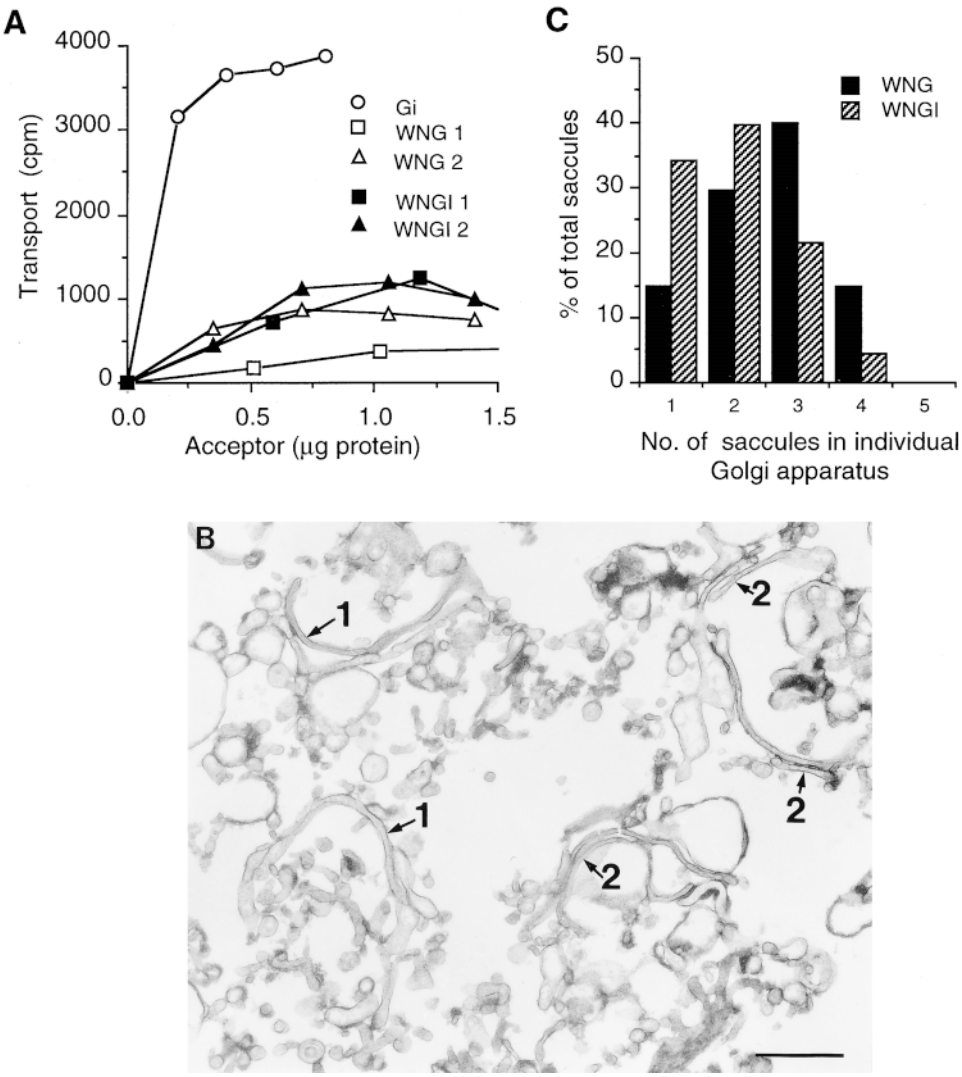

Figure 7. Imidazole-mediated unstacking of Golgi cisternae. Purified WNG fractions were gently incubated in 4 mM imidazole, pH 7.4, 0.25 M sucrose, and recovered as described in Materials and Methods. (A) Partial unstacking does not enhance acceptor activity. The indicated amounts of the parent and imidazole (I)-treated WNG fractions (WNGI) were compared with Gi fractions in the transport assay as described in Fig. 2 A. The GalT sp. act. for the WNG fractions were 11.6 and 12.5 mU, and for the WNGI fractions, 12.6 and 17.5 mU. (B) A representative micrograph of the WNGI fraction showing single (1) as well as double (2) cisternae. Although the cisternal membranes reveal greater access and free surfaces, there remains partial association with adjacent cisternae. Bar, 400 nm. (C) Morphometry of randomly sampled WNG or WNGI fractions reveals an increase in single cisternae after incubation in imidazole. A total of 89 (WNG) and 223 (WNGI) Golgi profiles were assessed as described in Materials and Methods.

tions could result from their specific SNARE content (Hay and Scheller, 1997; Nichols and Pelham, 1998), we measured the distribution of three SNAREs known to localize to the Golgi complex of mammalian cells: GS15 (Xu et al., 1997), GS28 (Subramaniam et al., 1996), and Vti-rp2 (Xu et al., 1998). Western blotting of fractions from a typical gradient identified all three v-SNARES in the transport active zone of the sucrose gradient (Fig. 12). GS15 was particularly enriched in active fractions, but could not be reliably quantified because it was detectable only by chemiluminescence. Quantitation of ^{125}I-labeled secondary antibodies with a Phosphorimager confirmed the high concentration of the other two SNAREs, especially GS28, in transport active fractions (Fig. 13). In conclusion, a GS15-enriched subcompartment of fragmented Golgi apparatus contained a minority of Golgi resident enzyme. This compartment, only releasable by physical fragmentation, appears responsible for the ability of this Golgi fraction to provide NAGT I in the cell-free transport assay.

Discussion

A combination of biochemical subcellular fractionation and morphological studies revealed an unexpected relationship between the extent of structural integrity of Golgi membranes and their ability to participate in fusion reactions leading to protein transport. These studies led to the identification of an active fusogenic fraction of defined SNARE content that can be released from inactive stacked preparations by vigorous homogenization in imidazole buffers.

This work took advantage of a novel procedure for the isolation of structurally intact hepatic Golgi fractions with greatly reduced endosomal contamination. This method exploited the significant size differences between these compartments by first using very gentle homogenization procedures to maintain the structural integrity of large Golgi complexes, followed by a low-speed centrifugation step to eliminate smaller endosomes. Golgi complexes were then resolved from ER, mitochondria, nuclei, and large plasmalemmal sheets (major contaminants of the parent pellet as identified by electron microscopy; Fazel, A., and J.J.M. Bergeron, unpublished observations) by density gradient floatation; the low density of hepatic Golgi complexes resulting from their enrichment in lipoprotein particles (Ehrenreich et al., 1973; Bergeron, 1979)

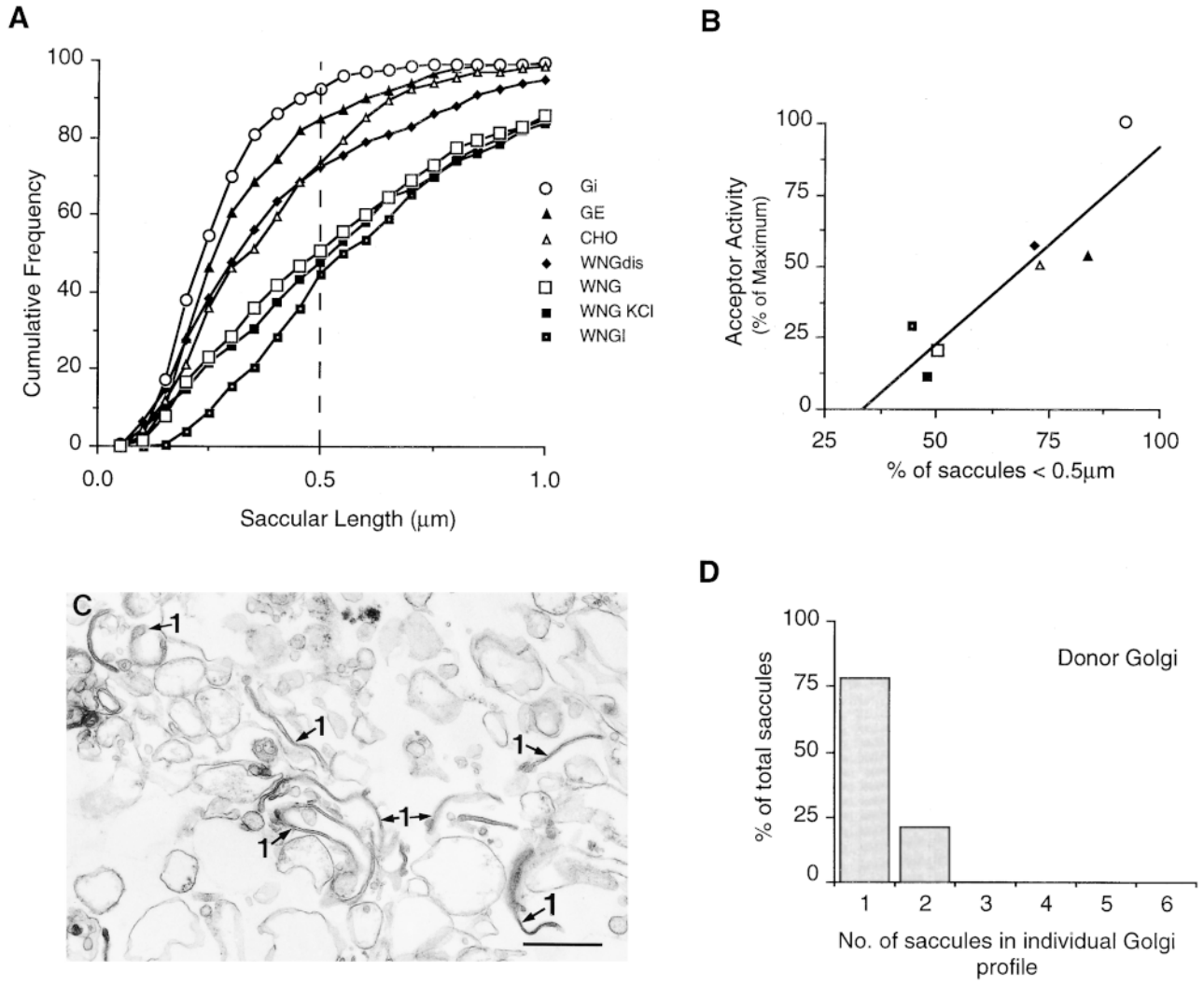

Figure 8. Morphometry of Golgi apparatus in hepatic and CHO fractions. (A) Saccular lengths were measured with a MOP III image analyzer and scored as their cumulative frequency. The dotted line represents the median cisternal length of the WNG fraction. (B) Correlation of acceptor activity with fragmentation. The frequencies were obtained from the intercepts with the dashed line of A, while the percent maximum transport was determined from the extent of transport measured with 0.8 μg of each fraction relative to that observed with a similar amount of the Gi fraction (100%). Simple linear regression (solid line) between saccular length and Golgi acceptor activity reveals a significant relationship with a coefficient of simple correlation ($r = 0.91$). To restrict the analysis to liver Golgi fractions, the point for CHO membranes (open triangle) was not used for this analysis, although the coefficient of regression remains unaltered if the point is included. (C) The VSV-G–containing donor Golgi fraction is fragmented and reveals a large number of short single saccular profiles (1). Bar, 400 nm. (D) Quantitation of 207 donor CHO Golgi profiles revealed 82% to be single cisternae.

facilitated this step. Morphological analysis of the resultant Golgi fraction revealed lipoprotein-filled stacked cisternae enriched in coated structures. Remarkably, cisternal lengths were much larger than those usually obtained, with 50% of the cisternae exceeding 0.5 μm and 20% exceeding 1.0 μm in length. Furthermore, in contrast to other Golgi fractions, >90% of the Golgi complexes were represented by stacked cisternae. Biochemical characterization revealed a marked reduction in endosomal contamination and a high enrichment in galactosyltransferase, ARF, and β-COP relative to hepatic or CHO Golgi fractions isolated by standard protocols. Because the yields achieved with this novel method are very similar to those obtained with standard methods, we conclude that WNG fractions do not represent an unusual subpopulation, but rather are highly representative of Golgi membranes in vivo.

Structurally Intact Golgi Fractions Are Inactive in The Cell-free Golgi Transport Assay

Love et al. (1998) previously established that the intra-Golgi cell-free transport assay measures transfer of NAGT I into VSV-G–containing cisternae (as opposed to vesicular transfer of VSV-G into NAGT I–containing cisternae), and proposed that this transfer involved small COP I vesicles. We therefore expected that highly stacked WT Golgi fractions with their elevated ARF and coatomer content would have the highest activity in the transport assay because they have abundant machineries for vesicle

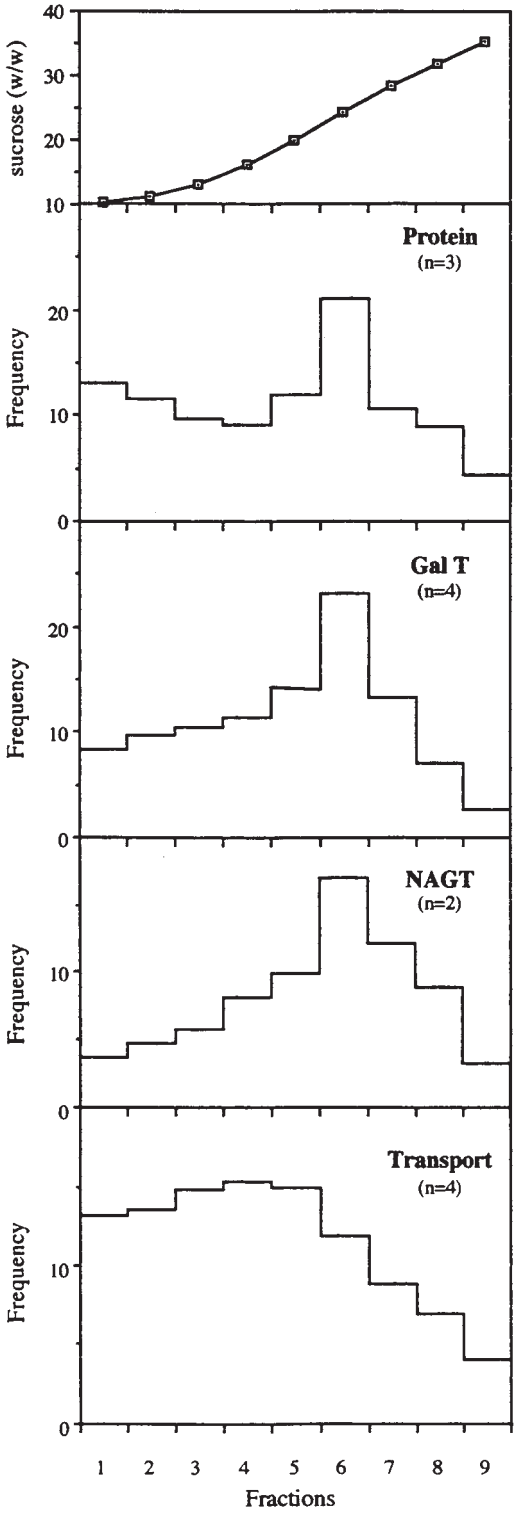

Figure 9. Rate-zonal separation of fusogenic active components of WNGdis. WNGdis preparations were loaded onto step sucrose gradients and analyzed by rate-zonal centrifugation as described in Materials and Methods. Each fraction was analyzed for sucrose and protein content, and GalT, NAGT, and transport activity. All assays were performed in duplicate under nonsaturating conditions. The number of fractionations is indicated in parentheses.

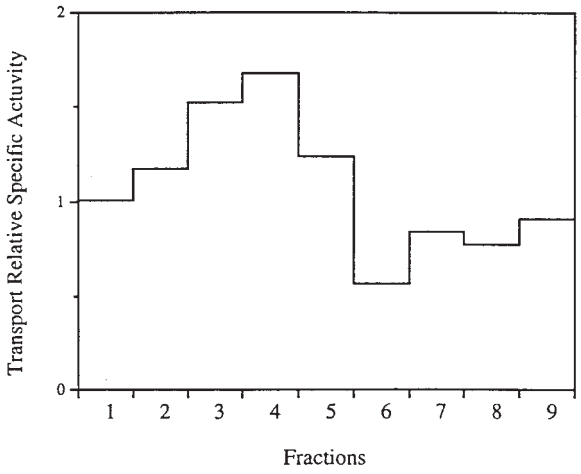

Figure 10. Transport-active components of WNGdis. The specific activity of transport competent components of the WNGdis fraction was calculated by dividing the values of transport activity (Fig. 9, bottom) over that of protein (Fig. 9, second panel). The highest concentration of transport-active acceptors is found in fraction 4. Similar results were obtained when normalizing transport activity to content of NAGT I.

budding. Unexpectedly, the WNG fraction was largely inactive as a source of NAGT I in this assay. This was in contrast to the greater transport activity of the more fragmented but demonstrably less pure fractions derived by standard procedures from wild-type CHO cells, or rat liver homogenates (Gi, GE fractions).

Several experiments ruled out trivial explanations for this lack of activity. Mixing experiments established that the low activity of the WNG fraction did not result from the presence of diffusible inhibitory factors, or the lack and/or consumption of diffusible limiting transport factors. The WNG fraction was not transport defective because it lacked cis-Golgi elements since p58, a marker of the intermediate compartment and cis-Golgi network (Lahtinen et al., 1996), was present at similar levels in Gi and WNG fractions. Moreover, lack of activity was not caused by overcoating of membrane because treatments that reduced (BFA) or eliminated (KCl wash) nearly all traces of COP I stably associated with WNG fractions did not increase the activity of stacked membranes in the assay. Finally, a budding assay confirmed that the WNG fraction was not biochemically inert since it could sort cargo and generate secretory vesicles (D. Shields and J.J.M. Bergeron, unpublished observations). We therefore conclude that the low activity of the WNG fraction in the Golgi transport assay is not an experimental artifact and instead reflects a defining feature of the cell-free assay relevant to the mechanism of cargo transport in vivo.

Isolation of Fusogenic Fragments from Stacked Golgi Fractions

Further analysis revealed that, whereas unstacking or removal of coatomer from WNG fractions had little effect on transport activity, homogenization in imidazole-containing buffers readily led to their activation for transport.

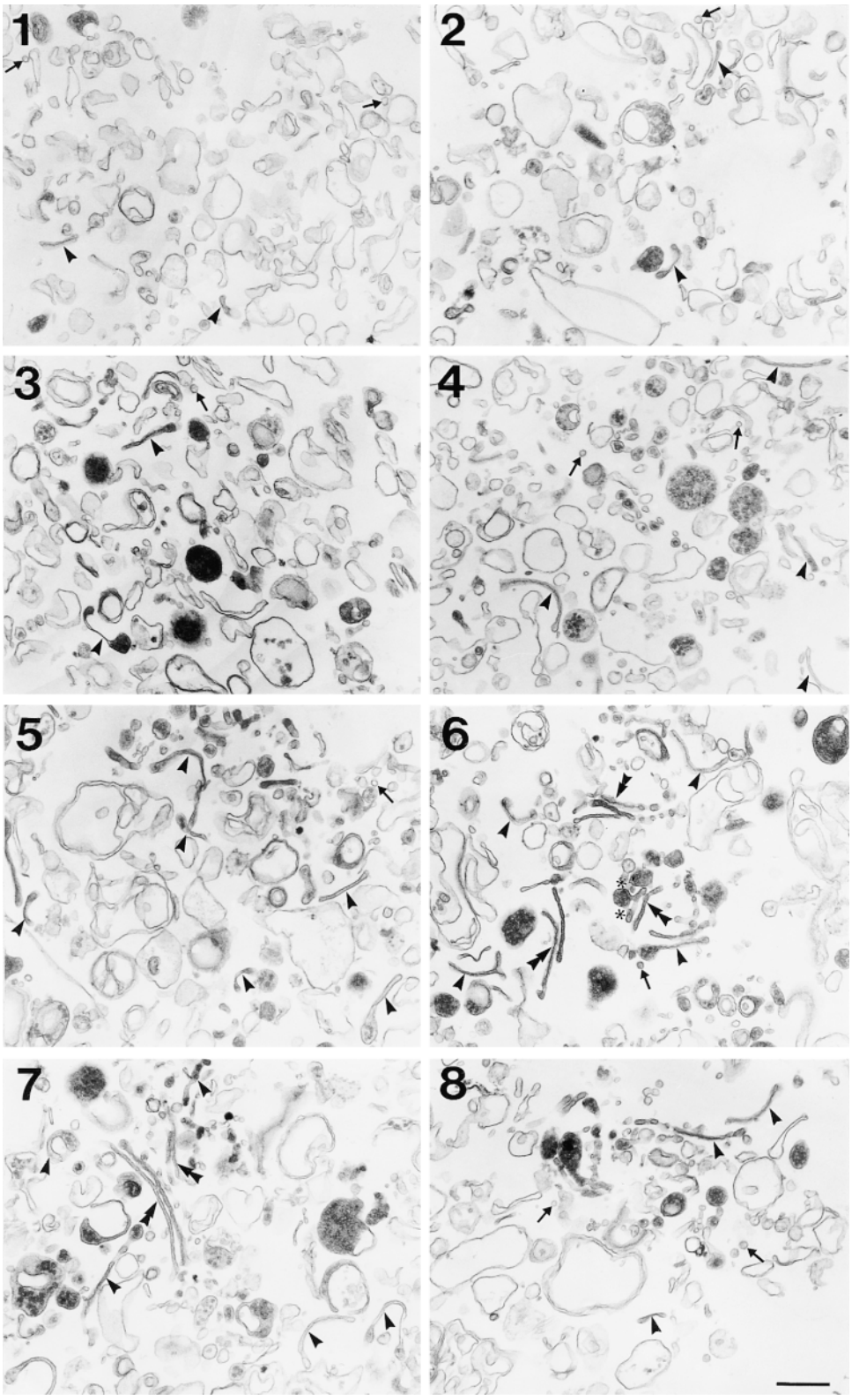

Figure 11. Morphology of WNG-dis rate-zonal subfractions. The subfractions from each portion of the gradient (fractions 1–8) of a typical fractionation (averaged in Fig. 9) were processed for random-sampling EM as described in Materials and Methods. A gradual increase in size in structures are found through fractions 1–8. Stacks made up of two saccules (double arrowheads) are found in fractions 6–8. Small vesicular profiles are also seen (small arrows), but throughout the gradient. Flattened cisternal elements of various lengths (arrowheads) are also frequent, especially in fractions 3–5 (arrowheads). A fortuitous section of a profile in fraction 6 reveals a continuity between two flattened cisternae and a lipoprotein-filled vesicular profile (*). Bar, 400 nm.

This activation could have resulted either from the release of tethered transport intermediates and/or fragmentation of fusogenic elements of cisternae, fenestrae, or intercisternal continuities. In the first case, the low activity of the WNG fraction would have resulted from a cytoskeletal matrix that restricted diffusion of transport intermediates but could be dislodged by homogenization. Recent tethering models for postulated intra-Golgi transport intermediates (Orci et al., 1998), as well as the demonstration of spectrin as part of a Golgi-associated cytoskeleton that includes microtubules and myosin (Beck and Nelson, 1998; Holleran and Holzbaur, 1998), provide likely candidates

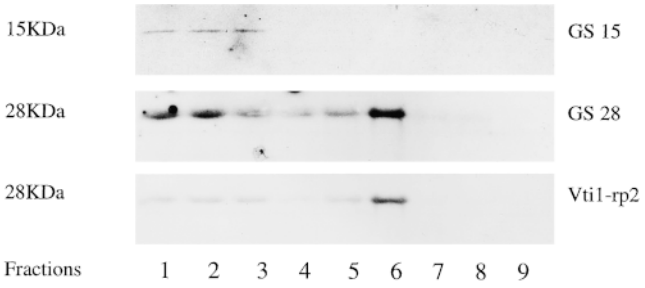

Figure 12. Distribution of GS15, GS28, and Vti1-rp2 in rate-zonal subfractions. A gradient was generated as for Fig. 9 and analyzed for content of GS15, GS28, and Vti1-rp2 by immunoblotting. Equal volumes of each fraction from the sucrose gradient (45 μl each) were evaluated. GS15 was visualized by chemiluminescence, while GS25 and Vti1-rp2 were detected using ^{125}I-labeled goat anti–mouse or ^{125}I goat anti–rabbit antibodies, respectively, followed by x-ray film exposure for 3 d. The mobilities of the respective antigens are indicated at left.

for this matrix. However, several observations suggested that such an explanation is unlikely. For example, neither washing in 0.3 M KCl (to remove matrices) or prior incubation at 4°C to depolymerize microtubules had any influence on the activity of WNG fractions in the cell-free transport assay. Furthermore, incubations in sucrose imidazole that did lead to cisternal unstacking and therefore liberation of a matrix did not enhance the transport activity of the WNG fraction.

More likely, our observations indicate that small Golgi-derived fragments play an important role as source of NAGT I in the assay, a possibility first suggested by the clear inverse correlation between average cisternal length and transport activity of various Golgi fractions (Figs. 3, 4 A, and 8). The demonstration, using rate-zonal centrifugation, that transport activity of a WNG fraction activated by homogenization in imidazole could be well resolved from the bulk of protein and sedimented less rapidly than more intact Golgi stacks and the peak of GalT or NAGT activities confirmed the importance of these fragments. (Figs. 9–13). Our results are in agreement with those of Love et al. (1998), who reported similar separation of a transport-active Golgi subfraction by velocity centrifugation from the bulk of larger (and less active) Golgi elements. Interestingly, the additional characterization of the transport active zone of our velocity gradients revealed a unique pattern of v-SNARES, especially GS15 and GS28, that could be relevant to their function in vivo. Antibodies to one of these, GS28, inhibited the same Golgi cell-free transport assay as used here (Nagahama et al., 1996), although a role in ER-to-Golgi transport has also been proposed (Subramaniam et al., 1996). The role of GS15 and Vti-rp2 in the cell-free transport assay remain to be elucidated. The exact nature of the fusogenic components in our fragmented Golgi fractions or the budded fraction of Love et al. (1998) remains unknown, but ongoing purification to morphological homogeneity should settle the morphological identity of the structures.

Previous work by Happe and Weidman (1998) established that the Golgi transport assay used here reconstitutes primarily heterotypic transfer between medial

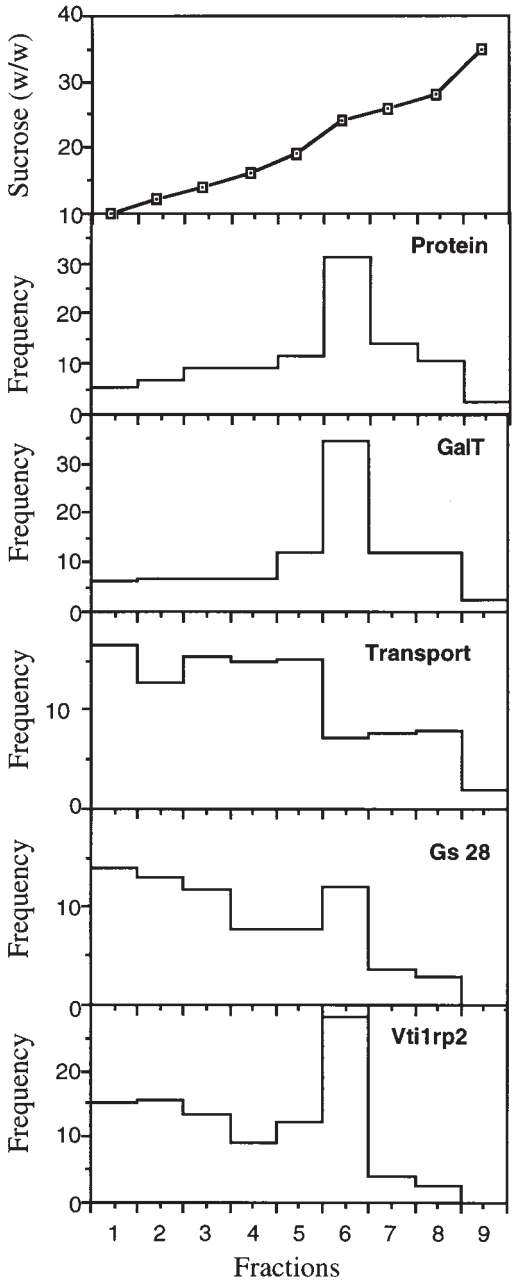

Figure 13. Rate-zonal centrifugation of Golgi v-SNARES in WNGdis subfractions. The gradient generated for Fig. 12 was analyzed for content of sucrose, total protein, GalT activity, and cell-free transport. The distribution of GS28 and Vti1-rp2 obtained by quantitative analysis of the immunoblot in Fig. 12 using a PhosphoImager (Fujix BAS1000 analyzer using a BASIII plate, Fuji) is also shown. Western blotting was repeated twice with a similar distribution observed.

NAGT I–containing Golgi compartments and an earlier (cis/ERGIC-located) VSV-G–containing one. Our studies are therefore unlikely to be explained by a homotypic fusion model akin to the reassembly of Golgi fragments after mitotic disassembly (Rabouille et al., 1995a,b) or pharmacological disassembly via ilimaquinone (Takizawa et al.,

1993; Acharya et al., 1995). Our homogenization protocol to release active fragments produced membranes of the same size and type as those normally recovered by the standard isolation procedures used by Happe and Weidman (1998) and others. In contrast, generation of mitotic kinases and IQ-induced fragments likely involves changes in membrane composition and/or properties that would not be reproduced by the simple physical forces used here.

The Role of the Fusogenic Compartment in Golgi Transport In Vivo

Several recent studies that established that the Golgi apparatus is a dynamic organelle undergoing constant remodeling actually predict the fusogenic fragments identified in our studies. Labeling of Golgi structures in living cells with a fluorescent sphingolipid precursor first revealed that the trans-Golgi elements of separate stacks readily form and break tubular interconnections (Cooper et al., 1990). Time-lapse photography of cells expressing green fluorescent protein–Golgi protein chimeras extended these studies and demonstrated dynamic extension/retraction of tubules that sometimes initiated novel and thicker connections between adjacent Golgi elements (Sciaky et al., 1997). These Golgi remodeling events have been proposed to contribute to Golgi traffic and help maintain the distribution of Golgi resident enzymes during rapid anterograde transport of secretory cargo through the organelle in vivo. Such observations suggest dynamic assembly of fusion sites such as uncoated bud tips and tubules readily observed by freeze-etch electron microscopy at the rims of cisternae (Weidman et al., 1993; Happe and Weidman, 1998) that could be preferentially recovered in a subset of the Golgi fragments generated during homogenization. The transport active fragments identified here and in the studies of Love et al. (1998) could therefore represent intra-Golgi intermediates involved in maintaining the distribution of Golgi resident enzymes during rapid anterograde transport of secretory cargo through the organelle in vivo.

Interestingly, Sciaky et al. (1997) also observed the retrograde transport of a small proportion of galactosyltransferase–green fluorescent protein chimeras to the ER. This latter event may very well be COP I dependent and could account for the observation of Love et al. (1998) that a small proportion of vesicular NAGT I can be generated from parent Golgi membranes in an ARF, COP I coatomer-dependent fashion. However, such structures would only be a minor proportion of transport-active components in the cell-free transport assay and represent that proportion of Golgi resident enzyme recycling to the ER rather than to early Golgi compartments.

A maturation model for secretory protein transport through the Golgi complex, with possible transient tubular connections between fusogenic elements to allow resident glycosyl transferase redistribution accommodates more readily the available data on the morphological characteristics and mechanisms of secretory cargo and resident enzyme dynamics in the Golgi complex from yeast to mammalian cells (Bannykh and Balch, 1997; Mironov et al., 1997; Sciaky et al., 1997; Pelham, 1998; Wooding and Pelham, 1998). The complete resolution of the enzymology of the Golgi cell-free transport assay and the precise identity of the fusogenic subcompartment identified here and in the studies of Love et al. (1998) should help define the molecular mechanisms and morphological framework for traffic within the secretory pathway (Bannykh and Balch, 1997).

This paper is dedicated to the memory of the late Dr. Wei Lai (see footnote 2). We also thank Scott Berger, as well as Drs. Kathryn Howell, Peggy Weidman, Ben Glick, Jacques Paiement, J. Ostermann, and Charlie Smith for multiple discussions and critical reading of the manuscript; Dr. Wanjin Hong kindly provided affinity-purified antibodies to Golgi SNARE proteins.

This study was supported by grants from the Medical Research Council of Canada (J.J.M. Bergeron and P. Melançon) and grant GM-43378 from the National Institutes of Health (P. Melançon). M. Dominguez was supported by a Hydro-Québec Fellowship from McGill University.

Received for publication 29 June 1998 and in revised form 25 March 1999.

References

Acharya, U., R. Jacobs, J.-M. Peters, N. Watson, M.G. Farquhar, and V. Malhotra. 1995. The formation of Golgi stacks from vesiculated Golgi membranes requires two distinct fusion events. *Cell.* 82:895–904.

Balch, W.E., W.G. Dunphy, W.A. Braell, and J.E. Rothman. 1984. Reconstitution of the transport of protein between successive compartments of the Golgi measured by the coupled incorporation of *N*-acetylglucosamine. *Cell.* 39:405–416.

Bannykh, S.I., and W.E. Balch. 1997. Membrane dynamics at the endoplasmic reticulum-Golgi interface. *J. Cell Biol.* 138:1–4.

Balch, W.E., and J.E. Rothman. 1985. Characterization of protein transport between successive compartments of the Golgi apparatus: asymmetric properties of donor and acceptor activities in a cell-free system. *Arch. Biochem. Biophys.* 240:413–425.

Baudhuin, P., P. Evrard, and J. Berthet. 1967. Electron microscopic examination of subcellular fractions. *J. Cell Biol.* 32:181–191.

Beck, K.A., and W.J. Nelson. 1998. A spectrin membrane skeleton of the Golgi complex. *Biochim. Biophys. Acta.* 1404:153–160.

Bergeron, J.J.M. 1979. Golgi fractions from livers of control and ethanol intoxicated rats: enzymic and morphologic properties following rapid isolation. *Biochim. Biophys. Acta.* 555:493–503.

Bergeron, J.J.M., R.A. Rachubinski, R.A. Sikstrom, B.I. Posner, and J. Paiement. 1982. Galactose transfer to endogenous acceptors within Golgi fractions from rat liver. *J. Cell Biol.* 92:139–146.

Bergeron, J.J.M., J. Paiement, M.N. Khan, and C.E. Smith. 1985. Terminal glycosylation in hepatic Golgi fractions: heterogenous locations for sialic acid and galactose acceptors and their transferases. *Biochim. Biophys. Acta.* 821: 393–403.

Bonfanti, L., A.A. Mironov, Jr., J.A. Martinez-Menarguez, O. Martella, A. Fusella, M. Baldassare, R. Buccione, H.J. Geuze, A. Mironov, and A. Luini. 1998. Procollagen traverses the Golgi stack without leaving the lumen of cisterna: evidence for cisternal maturation. *Cell.* 95:993–1003.

Borisy, G.G., J.M. Marcum, J.B. Olmsted, D.B. Murphy, and K.A. Johnson. 1975. Purification of tubulin and associated high molecular weight proteins from porcine brain and characterization of microtubule assembly in vitro. *Ann. NY Acad. Sci.* 253:107–132.

Bradford, M. 1976. A rapid and sensitive method for the quantification of microgram quantities of protein utilizing the principle of protein-dye binding. *Anal. Biochem.* 72:248–254.

Braell, W.A., W.E. Balch, D.C. Dobbertin, and J.E. Rothman. 1984. The glycoprotein that is transported between successive compartments of the Golgi in a cell-free system resides in stacks of cisternae. *Cell.* 39:511–524.

Clermont, Y., A. Rambourg, and L. Hewrmo. 1994. Connections between the various elements of the cis- and mid-compartments of the Golgi apparatus of early rat spermatids. *Anat. Rec.* 240:469–480.

Cooper, M.S., A.H. Cornell-Bell, A. Schernavsly, J.W. Dani, and S.J. Smith. 1990. Tubulovesicular processes emerge from *trans*-Golgi cisternae, extend along microtubules and interlink adjacent *trans*-Golgi elements into a reticulum. *Cell.* 61:135–145.

Dominguez, M., K. Dejgaard, J. Füllekrug, S. Dahan, A. Fazel, J.-P. Paccaud, D.Y. Thomas, J.J.M. Bergeron, and T. Nilsson. 1998. Gp25L/emp24/p24 protein family members of the *cis*-Golgi network bind both COP I and II coatomer. *J. Cell Biol.* 141:751–766.

Ehrenreich, J.H., J.J.M. Bergeron, P. Siekevitz, and G.E. Palade. 1973. Golgi fractions prepared from rat liver homogenates. I. Isolation procedure and morphological characterization. *J. Cell Biol.* 59:45–92.

Elazar, Z., L. Orci, J. Ostermann, M. Amherdt, G. Tanigawa, and J.E. Rothman. 1994. ADP-ribosylation factor and coatomer couple fusion to vesicle

budding. *J. Cell Biol.* 124:415–424.
Farquhar, M.G., and G.E. Palade. 1981. The Golgi apparatus (complex)-(1954–1981)-from artifact to center stage. *J. Cell Biol.* 91:77*s*–103*s*.
Farquhar, M.G., and G.E. Palade. 1998. The Golgi apparatus: 100 years of progress and controversy. *Trends Cell Biol.* 8:2–10.
Frank, B.H., D.E. Peavy, C.S. Hooker, and W.C. Duckworth. 1983. Receptor binding properties of monoiodotyrosyl insulin isomers purified by high performance liquid chromatography. *Diabetes.* 32:705–711.
Fries, E., and J.E. Rothman. 1980. Transport of vesicular stomatitis virus glycoprotein in a cell-free extract. *Proc. Natl. Acad. Sci. USA*. 77:3870–3874.
Gaynor, E.C., and S.D. Emr. 1997. COP I-independent anterograde transport: cargo selective ER to Golgi protein transport in yeast COP I mutants. *J. Cell Biol.* 136:789–802.
Glick, B.S., T. Elston, and G. Oster. 1997. A cisternal maturation mechanism can explain the asymmetry of the Golgi stack. *FEBS Lett.* 414:177–181.
Griffiths, G. 1996. On vesicles and membrane compartments. *Protoplasma.* 195: 37–58.
Happe, S., and P. Weidman. 1998. Cell-free transport to distinct Golgi cisternae is compartment specific and ARF-independent. *J. Cell Biol.* 140:511–524.
Hay, J.C., and R. Scheeler 1997. SNARES and NSF in targeted membrane fusion. *Curr. Biol*. 9:505–512.
Hayes, B.K., H.H. Freeze, and A. Varki. 1993. Biosynthesis of oligosaccharides in intact Golgi preparations from rat liver. *J. Biol. Chem*. 268:16139–16157.
Hayes, B.K., and A. Varki. 1993. Biosynthesis of oligosaccharides in intact Golgi preparations from rat liver. *J. Biol. Chem*. 268:16155–16169.
Ho, W.C., B. Storrie, R. Pepperkok, W. Ansorge, P. Karecla, and T.E. Kreis. 1990. Movement of interphase Golgi apparatus in fused mammalian cells and its relationship to cytoskeletal elements and rearrangement of nuclei. *Eur. J. Cell Biol.* 52:315–327.
Holleran, E.A., and E.L. Holzbaur. 1998. Speculating about spectrin: new insights into the Golgi-associated cytoskeleton. *Trends Cell Biol.* 8:26–29.
Klausner, R.D., J.G. Donaldson, and J. Lippincott-Schwartz. 1992. Brefeldin A: insights into the control of membrane traffic and organelle structure. *J. Cell Biol.* 116:1071–1080.
Lahtinen, U., U. Hellman, C. Wernstedt, J. Saraste, and R.F. Pettersson. 1996. Molecular cloning and expression of a 58-kDa *cis*-Golgi and intermediate compartment protein. *J. Biol. Chem*. 271:4031–4037.
Lippincott-Schwartz, J., N.B. Cole, and J. Presley. 1998. Unraveling Golgi membrane traffic with green fluorescent protein chimeras. *Trends Cell Biol.* 8:16–20.
Love, H.D., C.-C. Lin, C.S. Short, and J. Ostermann. 1998. Isolation of functional Golgi-derived vesicles with a possible role in retrograde transport. *J. Cell Biol.* 140:541–552.
Lowe, M., and T.E. Kreis. 1995. In vitro assembly and disassembly of coatomer. *J. Biol. Chem*. 270:31364–31371.
Malhotra, V., T. Serafini, L. Orci, J.C. Shepherd, and J.E. Rothman. 1989. Purification of a novel class of coated vesicles mediating biosynthetic protein transport through the Golgi stack. *Cell.* 58:329–336.
Melançon, P., B.S. Glick, V. Malhotra, P.J. Weidman, T. Serafini, M.L. Gleason, L. Orci, and J.E. Rothman. 1987. Involvement of GTP-binding "G" proteins in transport through the Golgi stack. *Cell.* 51:1053–1062.
Mellman, I., and K. Simons. 1992. The Golgi complex: in vitro veritas? *Cell.* 68: 829–840.
Mironov, A.A., P. Weidman, and A. Luini. 1997. Variations on the intracellular transport theme: maturing cisternae and trafficking tubules. *J. Cell Biol.* 138: 481–484.
Nagahama, M., L. Orci, M. Ravazzola, M. Amherdt, L. Lacomis, P. Tempst, J.E. Rothman, and T.H. Sollner. 1996. A v-SNARE implicated in intra-Golgi transport. *J. Cell Biol.* 133:507–516.
Nichols, B.J., and H.R.B. Pelham. 1998. SNARES and membrane fusion in the Golgi apparatus. *Biochim. Biophys. Acta.* 1404:9–31.
Orci, L., B.S. Glick, and J.E. Rothman. 1986. A new type of coated vesicular carrier that appears not to contain clathrin: its possible role in protein transport within the Golgi stack. *Cell*. 46:171–184.
Orci, L., M. Stamnes, M. Ravazzola, M. Amherdt, A. Perrelet, T.H. Sollner, and J.E. Rothman. 1997. Bidirectional transport by distinct populations of COP I-coated vesicles. *Cell.* 90:335–349.
Orci, L., A. Perrelet, and J.E. Rothman. 1998. Vesicles on strings: morphological evidence for processive transport within the Golgi stack. *Proc. Natl. Acad. Sci. USA*. 95:2279–2283.
Ostermann, J., L. Orci, K. Tani, M. Amherdt, M. Ravazzola, Z. Elazar, and J.E. Rothman. 1993. Stepwise assembly of functionally active transport vesicles. *Cell*. 75:1015–1025.
Paiement, J., and J.J.M. Bergeron. 1983. Localization of GTP-stimulated core glycosylation to fused microsomes. *J. Cell Biol.* 96:1791–1796.
Palade, G. 1975. Intracellular aspects of the process of protein secretion. *Science.* 189:347–358.
Palade, G.E. 1983. Membrane biogenesis: an overview. *Methods Enzymol.* 96: xxix–lv.
Pelham, H.R. 1998. Getting through the Golgi complex. *Trends Cell Biol.* 8:45–49.
Rabouille, C., T. Misteli, R. Watson, and G. Warren. 1995a. Reassembly of Golgi stacks from mitotic Golgi fragments in a cell-free system. *J. Cell Biol.* 129:605–618.
Rabouille, C., T.P. Levine, J.M. Peters, and G. Warren. 1995b. An NSF-like ATPase, p97, and NSF mediate cisternal regrowth from mitotic Golgi fragments. *Cell.* 82:905–914.
Rothman, J.E., R.L. Miller, and L.J. Urbani. 1984. Intercompartmental transport in the Golgi complex is a dissociative process: facile transfer of membrane protein between two Golgi populations. *J. Cell Biol.* 99:260–271.
Rothman, J.E., and L. Orci. 1992. Molecular dissection of the secretory pathway. *Nature*. 355:409–415.
Rothman, J.E. 1996. The protein machinery of vesicle budding and fusion. *Protein Sci.* 5:182–194.
Rothman, J.E., and F.T. Wieland. 1996. Protein sorting by transport vesicles. *Science.* 272:227–234.
Sciaky, N., J. Presley, C. Smith, K.J. Zaal, N. Cole, J.E. Moreira, M. Terasaki, E. Siggia, and J. Lippincott-Schwartz. 1997. Golgi tubule traffic and the effects of Brefeldin A visualized in living cells. *J. Cell Biol.* 139:1137–1155.
Schekman, R., and I. Mellman. 1997. Does COPI go both ways? *Cell.* 90:197–200.
Schnepf, E. 1993. Golgi apparatus and slime secretion in plants: the early implications and recent models of membrane traffic. *Protoplasma.* 172:3–11.
Serafini, T., L. Orci, M. Amherdt, M. Brunner, R.A. Kahn, and J.E. Rothman. 1991. ADP-ribosylation factor is a subunit of the coat of Golgi-derived COP-coated vesicles: a novel role for a GTP-binding protein. *Cell.* 67:239–253.
Simionescu, N., and M. Simionescu. 1976. Galloylglucoses of low molecular weight as mordant in electron microscopy. *J. Cell Biol.* 70:608–621.
Smith, C.E., J. Paiement, and J.J.M. Bergeron. 1986. Subcellular distribution of acid NADPase activity within the parenchymal cells of rat liver. *J. Histochem. Cytochem.* 34:649–658.
Smith, D.E., and P.A. Fisher. 1984. Identification, developmental regulation, and response to heat shock of two antigenically related forms of a major nuclear envelope protein in *Drosophila* embryos: application of an improved method for affinity purification of antibodies using polypeptides immobilized on nitrocellulose blots. *J. Cell Biol.* 99:20–28.
Subramaniam, V.N., F. Peter, R. Philip, S.H. Wong, and W. Hong. 1996. GS28, a 28-kilodalton Golgi SNARE that participates in ER-Golgi transport. *Science.* 272:1161–1163.
Takizawa, P.A., J.K. Yucel, B. Veit, D.J. Faulkner, T. Deerinch, G. Soto, M. Elliman, and V. Malhotra. 1993. Complete vesiculation of Golgi membranes and inhibition of protein-transport by a novel sea sponge metabolite, ilimaquinone. *Cell.* 73:1079–1090.
Taylor, T.C., R.A. Kahn, and P. Melançon. 1992. Two distinct members of the ADP-ribosylation factor family of GTP-binding proteins regulate cell-free intra-Golgi transport. *Cell.* 70:69–79.
Taylor, T.C., M. Kanstein, P. Weidman, and P. Melançon. 1994. Cytosolic ARFs are required for vesicle formation but not for cell-free intra-Golgi transport: evidence for coated vesicle-independent transport. *Mol. Biol. Cell.* 5:237–252.
Vischer, P., and R.C. Hughes. 1981. Glycosyl transferase of baby-hamster-kidney (BHK) cells and ricin-resistant mutants. *Eur. J. Biochem*. 117:275–284.
Waters, M.G., T. Serafini, and J.E. Rothman. 1991. 'Coatomer': a cytosolic protein complex containing subunits of non–clathrin-coated Golgi transport vesicles. *Nature*. 349:248–254.
Weidman, P.J. 1995. Anterograde transport through the Golgi complex: do Golgi tubules hold the key? *Trends Cell Biol.* 5:302–305.
Weidman, P.J., P. Melançon, M.R. Block, and J.E. Rothman 1989. Binding of an *N*-ethylmaleimide-sensitive fusion protein to Golgi membranes requires both a soluble protein(s) and an integral membrane receptor. *J. Cell Biol.* 108:1589–1596.
Weidman, P., R. Roth, and J. Heuser. 1993. Golgi membrane dynamics imaged by freeze-etch electron microscopy: views of different membrane coating involved in tubulation versus vesiculation. *Cell.* 75:123–133.
Whitney, J.A., M. Gomez, D. Sheff, T.E. Kreis, and I. Mellman. 1995. Cytoplasmic proteins involved in endosome function. *Cell.* 83:703–713.
Wooding, S., and H.R.B. Pelham. 1998. The dynamics of Golgi protein traffic visualized in living yeast cells. *Mol. Biol. Cell.* 9:2667–2680.
Xu, Y., S.H. Wong, T. Zhang, V.N. Subramaniam, and W. Hong. 1997. GS15, a 15-kilodalton Golgi soluble *N*-ethylmaleimide–sensitive factor attachment protein receptor (SNARE) homologous to rbet1. *J. Biol. Chem*. 272:20162–20166.
Xu, Y., S.H. Wong, B.L. Tang, V.N. Subramaniam, T. Zhang, and W. Hong. 1998. A 29-kilodalton Golgi soluble *N*-ethylmaleimide–sensitive factor attachment protein receptor (Vti1-rp2) implicated in protein trafficking in the secretory pathway. *J. Biol. Chem*. 273:21783–21789.